Cytometry 28:305–310 (1997)

Automatic Analysis of Growth Onset, Growth Rate and Colony Size of Individual Bone Marrow Progenitors

J. Boezeman,[1,2]* R. Raymakers,[1,2] G. Vierwinden,[2] and P. Linssen[2]

[1]Division of Hematology, University Hospital Nijmegen, Nijmegen, The Netherlands
[2]Central Hematology Laboratory, University Hospital Nijmegen, Nijmegen, The Netherlands

Received 23 July 1996; Accepted 5 April 1997

A method for automatic enumeration of proliferating bone marrow progenitors after single cell sorting is described. The system is based on regular inverse microscopy, recording with a video camera, and image analysis using dedicated software on an Apple computer. Single CD34+ progenitor cells were sorted in 96-well plates. Three times weekly phase-contrast video images of each well were stored and analyzed for the actual number of cells. From the subsequent counts growth curves were plotted for each individual progenitor. Enumeration by image analysis correlated very well with manual cell counting ($r = 0.99$, $P < 0.0001$). To show the capability of the method to analyze growth rate and growth delay, more differentiated (CD34+/CD13+/CD33+) progenitors were compared with more primitive (CD34+/CD13+/CD33g−) progenitors. Differences in the timing of colony outgrowth were shown to be based on delay in growth initiation. Initiation of growth was delayed 2.6–3.1 days in CD34+/CD13+/CD33− fraction of 3 different donors ($P < 0.0001$). The growth rates of the progenitors in both fractions were not significantly different. The described method seems important to more accurately evaluate subpopulations of progenitors, the effect of growth promoting or inhibiting factors, and effects of cytotoxic drugs and irradiation. Cytometry 28:305–310, 1997. © 1997 Wiley-Liss, Inc.

Key terms: image analysis; single cell culture; CD34

The established method to quantitate the proliferative capacity of single cells is a clonogenic assay in semi-solid medium. A known number of immobilized cells are plated and after a fixed incubation time (mostly 7–14 days) the number of aggregates are counted. The plating efficiency, defined as the percentage of cells giving rise to a colony (>40–50 cells) or cluster (2–40 or 50 cells) is then calculated. The colony size reflects the clonogenic capacity of the original progenitor cell at the time of evaluation.

Image analysis has been used to enumerate the number of aggregates (4, 5). Time-lapse video images allowed dynamic descriptions of the growth in the assay (2, 3). Slocum and co-workers developed a method to monitor and evaluate the growth history of individual cells plated in semi-solid medium (6–8). The technique is based on measurement of the colony diameter using pseudo dark field microscopy and thus limited to more or less coherent, non-overlapping aggregates. Hematopoietic progenitors are characterized by a low plating efficiency ($<10^{-3}$) and the tendency of the colonies to spread and mix with non-proliferating cells and nearby colonies. In this paper we describe a method to evaluate the growth of individual human hematopoietic progenitors after single cell sorting by flow cytometry. Tracking the growth of individual cells allows evaluation of more sophisticated parameters such as delayed onset of growth and variance of growth rate.

The growing colonies result in low-contrast images with hardly any intensity edges marking the individual cells of the colony. In bright phase contrast microscopy, the pronounced edges of the objects are the targets for the segmentation routines. With well-chosen parameters and discrimination from noisy and false objects, the segmentation routines recognized individual cells, both within the aggregate as well as cells that drifted away from the aggregate. Furthermore, cells can be picked from individual wells and analyzed for differentiation markers, PCR or cell morphology after staining of cytospin preparations.

To illustrate the method, normal human bone marrow CD34 positive cells were used. After sequential analysis, growth curves for individual wells could be constructed. In immunophenotypically more primitive subpopulations, growth delay was observed although growth rates were within restricted limits.

MATERIALS AND METHODS

Bone Marrow CD34+ Cells

Bone marrow cells were obtained from healthy bone marrow donors after informed consent. Anti-CD34 (BI3C5)

*Correspondence to: J. Boezeman, Division of Hematology 544, University Hospital Nijmegen, PO Box 9101, 6500 HB Nijmegen, The Netherlands.
E-mail: J.Boezeman@chl.azn.nl

directly coated on M-450 paramagnetic beads as well as Detach-a-Bead were purchased from Dynal (Oslo, Norway).

Media, Cultureware, and Monoclonal Antibodies

Media and cultureware consisted of Iscove's medium (Flow Laboratories, Irvine, Scotland), fetal bovine serum (FBS, Hyclone, Logan, UT) and recombinant growth factors, G-CSF and SCF (a gift from Amgen, Thousand Oaks, CA), GM-CSF (a gift of Dr. E. Liehl, Sandoz Forschungsinstitut, Vienna, Austria), erythropoietin (1.5 U/ml) (Eprex, Cilag BV, Beerse, Belgium), penicillin 50 U/ml, streptomycin 50 µg/ml (Flow Laboratories), deionized bovine serum albumin (BSA) (Sigma, St. Louis, MO), human transferrin (Sigma), and 2-β-mercaptoethanol (Merck, Darmstadt, Germany). Roundbottom 96-well plates (Costar 3799, Cambridge, MA) were used.

Directly labelled antibodies anti-CD33-PE (My-9, Becton-Dickinson, Oxnard, CA) and anti-CD13-FITC (WM-47, Dako, Glostrup, Denmark) were used for sorting. To check for purity, the CD34+ fraction was labeled with HPCA-2-PE (Becton-Dickinson).

Bone Marrow Samples

Nucleated cells were isolated by Ficoll (Sigma) 1.077 g/ml centrifugation. After washing twice in buffer interphase, cells were incubated with anti-CD34-coated paramagnetic beads (cell:bead ratio 2:1, in 1 ml buffer) for 45 min at 4°C. By magnetic separation (8 wash steps) the rosetted cells were isolated. To remove the beads, the cells (in 100 µl buffer) were diluted with Detach-a-Bead (10 µl/10^6 cells), for 60 min at room temperature. The beads were removed in 3 wash steps with a magnet, the cells resuspended in Iscove's medium with 10% (v/v) fetal bovine serum and 15 U/ml preservative free heparin at a cell concentration of about 2×10^5 cells/ml. This cell suspension was diluted 1:1 with medium containing 20% DMSO (v/v) on ice. The cells were cryopreserved (Kryo 10; PlanerBiomed, Sunbury, Middlesex, UK) in 2-ml freezing tubes and stored at −198°C.

Thawing and Labeling of Bone Marrow Cells

The vials were thawed in a 37°C waterbath, and diluted in FBS, containing 0.02 mg/ml DNAse (deoxyribonuclease I, grade II, from bovine pancreas, Boehringer-Mannheim, Mannheim, FRG) and 4M MgSO4 and 15 U/ml preservative-free heparin. After washing, the cell pellet was incubated for 30 min at 4°C with 100 µl of diluted monoclonal antibodies in 10% pooled human serum: anti-CD13-FITC 1:20 and anti-CD33-PE 1:20.

Flow Cytometric Single Cell Sorting

The labeled cells were sorted by a Coulter (Hialeah, FL) Epics Elite Flow cytometer equipped with an autoclone unit. The 40-mW Argon ion laser was running at 15 mW and emitting at 488 nm. Dichroic mirrors of 550 and 625 nm and band pass filters 525/40 and 575/30 were used. A gate in the forward vs. right angle light scatter diagram was used to exclude dead cells and debris. To standardize for fluorescence intensity, commercially available green and red fluorescent beads (Calibrite, B&D, San Jose, CA) were used.

Culturing Conditions of the Single Cells in 96-Well Plates

Single cells were sorted in roundbottom 96-well plates, pre-filled with 50 µl liquid medium, consisting of Iscove's, penicillin 50 U/ml, streptomycin 50 µg/ml (Flow Laboratories) with 20% FBS, 5% deionized bovine serum albumin (BSA), 0.3 mg/ml human transferrin, and 5×10^{-5} M 2-β-mercaptoethanol. Recombinant growth factors were added: G-CSF (20 ng/ml), SCF (25 ng/ml), IL-3 (50 ng/ml), GM-CSF (20 ng/ml), IL-6 (10 ng/ml) and erythropoietin (1.5 U/ml). To reduce false background objects such as crystals and fibers, the complete medium was filtered through a 0.2 µm Millipore (Bedford, MA) filter. After sorting, the plates were placed in an incubator at 37°C, 5% CO_2, in a fully humidified atmosphere and evaluated on days 4, 6, 8, 11, 13, 15, and 18.

Image System

The images were acquired on a Zeiss (Thornwood, NY) Axiovert 35M inverted microscope equipped with the 10×/0.3 Ph1 bright phase contrast objective and digitized in 512 × 512 × 8 with a HCS MX5 black and white video camera (DIFA, Breda, The Netherlands) coupled with the Pixel Pipeline in a Macintosh-IIfx. The spatial resolution was defined by pixel size and the magnification of the objective was 1.3 µm. The resulting field size was 720 × 720 µm. The plates were positioned in X, Y, and Z directions with a EK8b MTP scanning table (Marzhauser, Wetzlar, Germany) controlled either by the serial interface of the Mac or manually by the operator. As X and Y centering of the well was less critical, the final adjustment of the focal plane was essential for the correct contour detection. The segmentation algorithms were developed with the TCL-image package.

Segmentation

The algorithm has essentially three steps. The image was first high pass filtered, with filter size 7 × 7 to enhance the cell-like objects. Introducing a threshold at low level resulted in potential cell objects. As the edges of cells sometimes disappeared between neighbors in the colony, a closing step was essential to allow broken contours to become contiguous. All non-circular objects with an aspect ratio >1.5 were then removed as well as the objects with an apparent inner space larger than 32 pixels, outside the normal cell size range. To determine the efficacy of the segmentation each scored object was marked with a centered dot.

Data Analysis

The final number of cells at the last day of counting discriminates between wells with growth (defined as >10 cells) or no growth (0–10 cells). Growth curves of the positive wells were plotted from the successive time views of the expanding colony. The phase of the growth curve

Table 1
Growth in Single Cell Assay[a]

	No. of wells with aggregates				Morphology aggregates >500 cells		
	>10 cells	>50 cells	>500 cells	>5,000 cells	GM	Erythroid	GEMM
CD13+/CD33−	66	57	49	33	67	14	18
CD13+/CD33+	68	50	28	11	89	4	7
CD13−/CD33−	40	34	25	6	8	80	12

[a]The numbers represent the wells which cumulatively showed >10, >50, >500, and >5,000 cells. The morphology distribution of the aggregates >500 cells is given. GM: granulocytic-monocytic; GEMM: granulocytic, erythroid, monocytic, and megakaryocytic. Presented data are a typical example of normal CD34+ selected bone marrow cells. For each phenotypic fraction one 96-well plate was sorted.

where the colony was in the range of 20–2,000 cells was selected for further analysis. Within this range the cells could be analyzed as single cells, not passing the image borders nor piling up. The selected phase was parametrized for the growth rate and the growth delay, where the latter was defined as the time point the growth curve passed the 600-cell point.

Statistical Analysis

The Mann Whitney and Pearson were applied for statistical analysis of the results.

RESULTS

Single Cell Sorting and Cloning in 96-Well Plates

Positive selection with immunomagnetic beads resulted in a >95% pure population of CD34 cells, which was checked by secondary labeling with HPCA-2-PE. Labeling of the CD34+ cells with CD33 and CD13 resulted in a characteristic pattern: a population of double positive cells (CD13+/CD33+), a double negative population, enriched for CD19+ (non-clonogenic in the applied culture system) cells and erythroid progenitors (CD13−/CD36+) (labels not shown) and a CD13+/CD33− population. Almost no CD13−/CD33+ cells were observed. The data of a typical example of growth in single cell assay is presented in Table 1. The cumulative number of wells with >10, >50, >500, and >5,000 cells are given for the three different immunophenotypic fractions. For the wells with >500 cells the colonies were analyzed for morphology. The CD13+/CD33− population was enriched for large colonies (>5,000 cells) of mixed, erythroid, and myeloid morphology. The CD13+/CD33+ colonies were smaller and predominantly of myeloid origin. The CD13−/33-fraction was enriched for smaller erythroid colonies. The CD13+/CD33− and the CD13+/33+ fractions were used in further experiments for growth rate and growth delay analysis. As immediately after sorting most cells float in the medium, single-cell deposit was checked by microscopic inspection 24 h after sorting, when the cells had sedimented into the center of the round bottom well. In >90% of the wells, a single cell was detectable on the bottom after 24 h.

Capturing Growth of Single Cells in 96-Well Plates

Capturing of images was started at day 4. A typical series of images from a single well is presented in Figure 1. From day 4 to 8 all cells had a blast-like appearance, which means a symmetrical, round cell shape. At day 11 the cells started to differentiate from the outer border of the colony; the round shape disappeared and the cells spread centrifugally. In this example at day 15 all cells were differentiated and no further cell divisions were observed. Typically, the initial process of "blast" cell proliferation was followed by differentiation starting from the outer border of the colony. A large variation was seen in the initial start of proliferation, the day differentiation began, and the final size of the colony (data not shown). In general, the larger the colonies the later differentiation started after the growth was initiated. Differentiation into myeloid and monocytic colonies was characterized by change in the shape of the cells and migration over the bottom. Erythroid colonies stayed compact, and differentiation was characterized by extrusion of the nucleus. Differentiation was checked by picking individual colonies and analyzing morphology on cytospin slides or immunophenotype after labeling for differentiation markers on the flow cytometer (CD14, CD15, and glycophorin).

Check on Segmentation by Correlation With Manual Counting and Marking Cells

Growth is defined when more than 10 objects are detected in the well. The low threshold of 10 ignores some artifacts in empty images, while growing colonies are not be missed. Table 2 compares the plating efficiency as evaluated by the system vs. manual operation. With 377 wells evaluated, false positivity was below 4%, false negativity below 2%. False positive events were related to wells where growth was initiated but stopped after 1–3 cell divisions. The segmentation algorithm was also evaluated by comparison with manual counting by a practiced operator. Figure 2 illustrates the large correlation ($r > 0.99$, $P < 0.0001$) over a wide range of colony sizes (1–169). A second check on correct segmentation by image analysis was done by marking each object recognized with a centered dot. Most of the background due to small particles and crystals in the medium could be reduced by filtration of the complete culture medium through a 0.2 μm Millipore filter. Segmentation was less accurate once the cells started to differentiate and lost their round shape appearance.

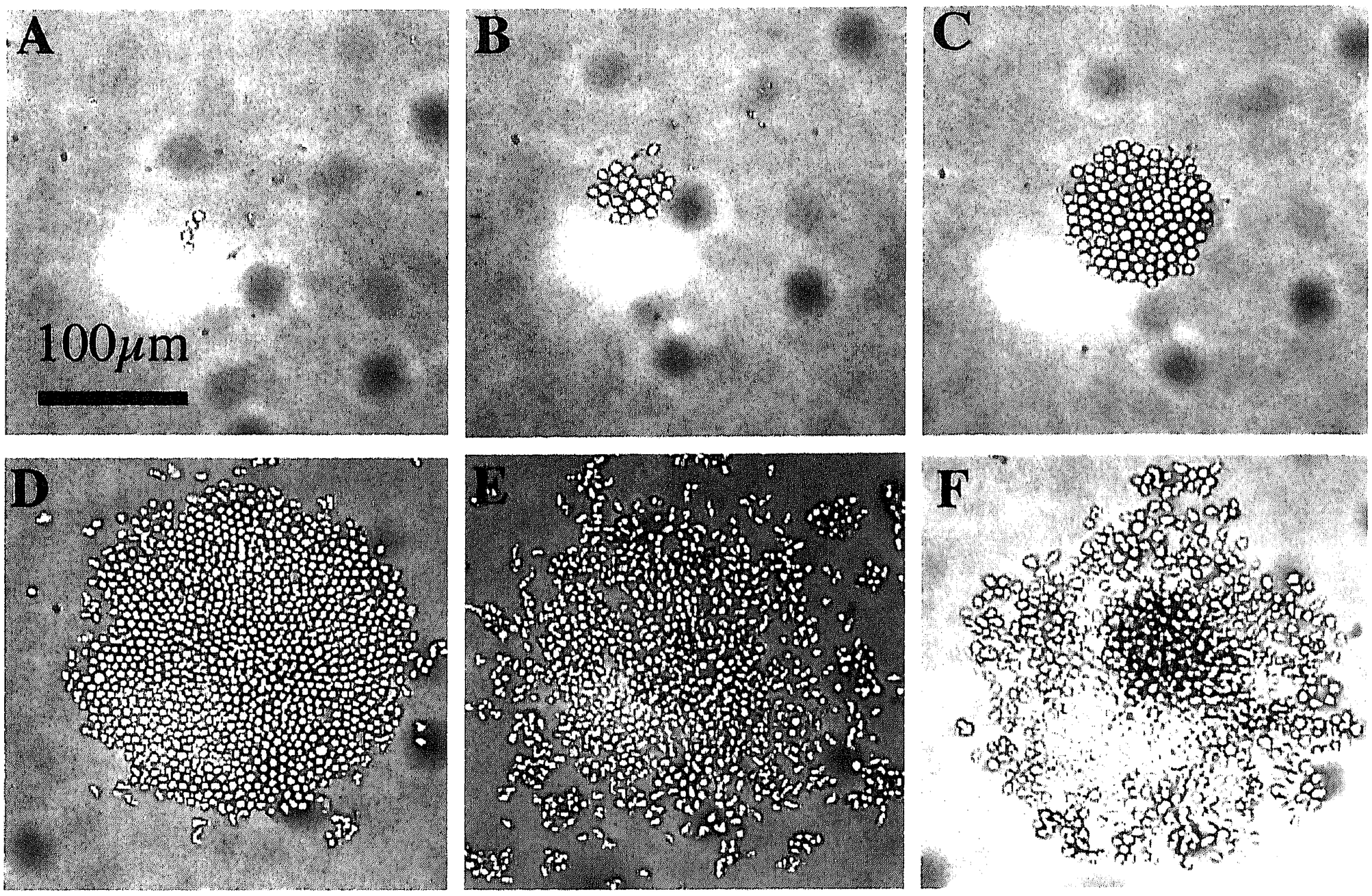

FIG. 1. Expansion and dispersion of a single cells derived myeloid colony at days 4, 6, 8, 11, 15, and 18. **A–C:** Cell number increases, but the cells remain round, blast-like cells. **D:** Cells at the border of the colony start to differentiate (day 11). This becomes more obvious in **E** and **F**. Differentiation is characterized by changes in cell morphology. The cells in this example start to disperse from day 11 onward.

Table 2
Comparison of Plating Efficiency Evaluated by Manual and Automatic Counting of Wells With >10 Cells[a]

	Manual		
Automatic	Yes	No	Total
Yes	159	14	173
No	4	200	204
Total	163	214	377

[a]Yes: more than 10 cells; No: less than 10 or no cells.

Analysis of Growth Curves of CD34+/13+/33+ and CD34+/13+/33− Sorted Cells

Growth curves were constructed for each separate well, thus for each individually sorted cell. Figure 3 shows three panels of curves from different 96-well plates, sorted with respect to the time the colony reached the 600-cell size. Figure 3A and B show the eight most fast-growing colonies, examples of CD34+/13+/33+ (Fig. 3A) and the CD34+/13+/33− (Fig. 3B) phenotypic fractions. Within these panels the variation in growth rates was not different for the two fractions: mean growth rate in A was 1.1 ± 0.04 and in B 1.1 ± 0.1. Although each curve per definition

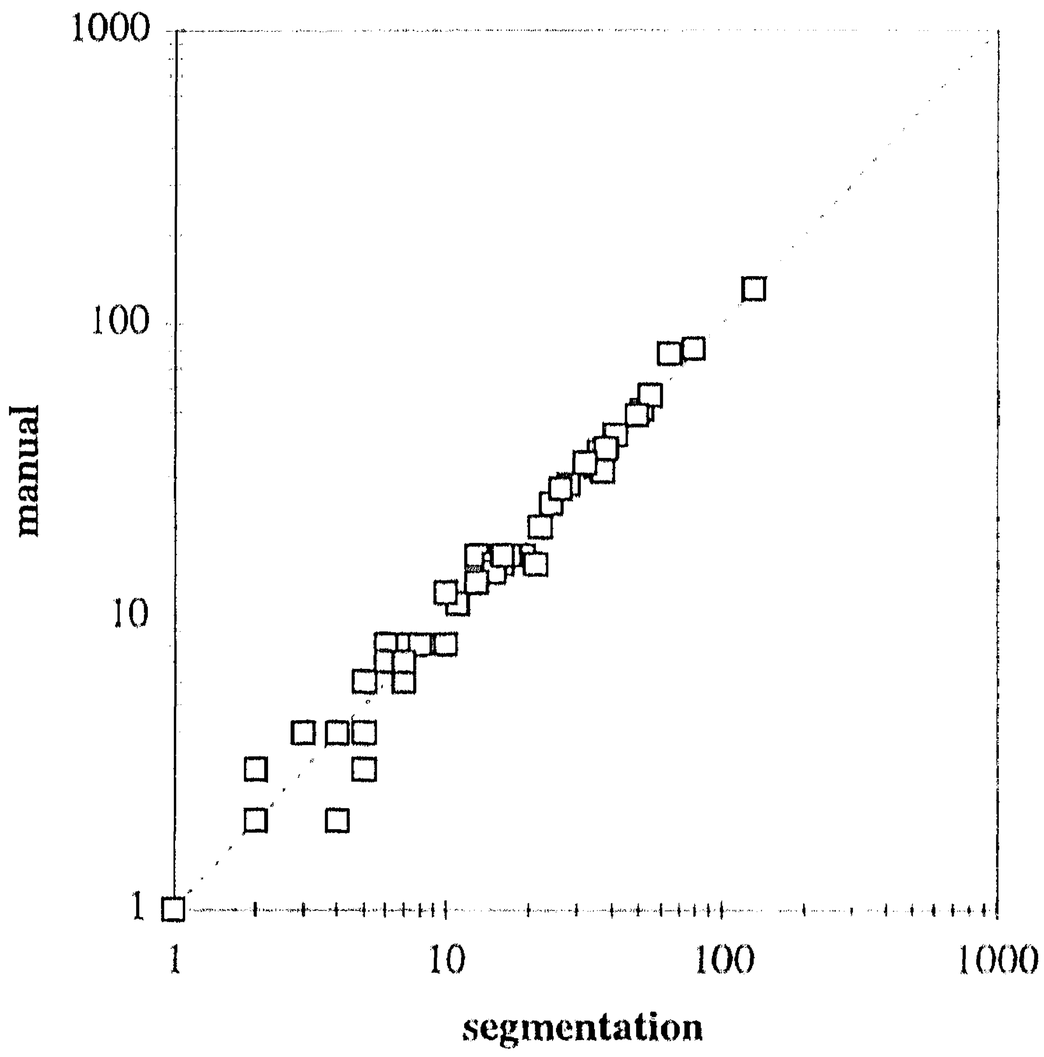

FIG. 2. Comparison of the number of cells/well by manual vs. automatic counting. Manual counting was done by one practiced technician. The correlation coefficient was $r = 0.99$ ($P < 0.0001$).

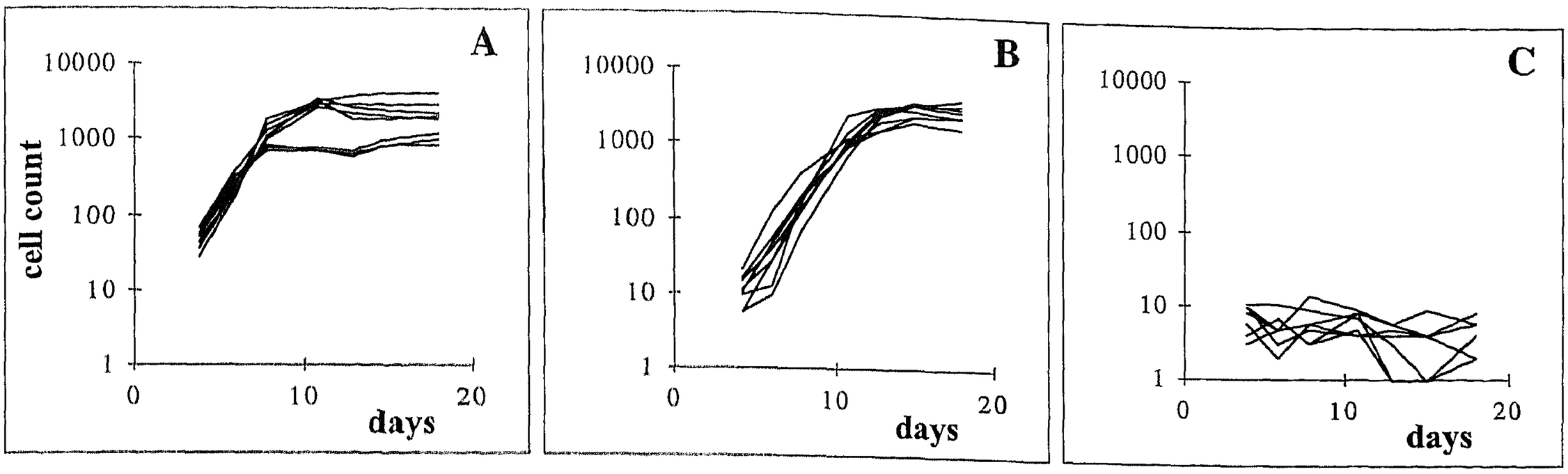

FIG. 3. Plotted growth curves, each curve representing a single well. The curves were sorted for the fastest growth rates. A and B show the most fast-growing colonies. **A:** CD13+/CD33+ cells. **B:** CD13+/CD33− cells. In A the individual growth curves show more overlap than in B, which is due to growth delay in the CD13+/CD33− fraction, while the slopes of the growth curves in A and B are not different. **C:** Growth curves of wells with no growth.

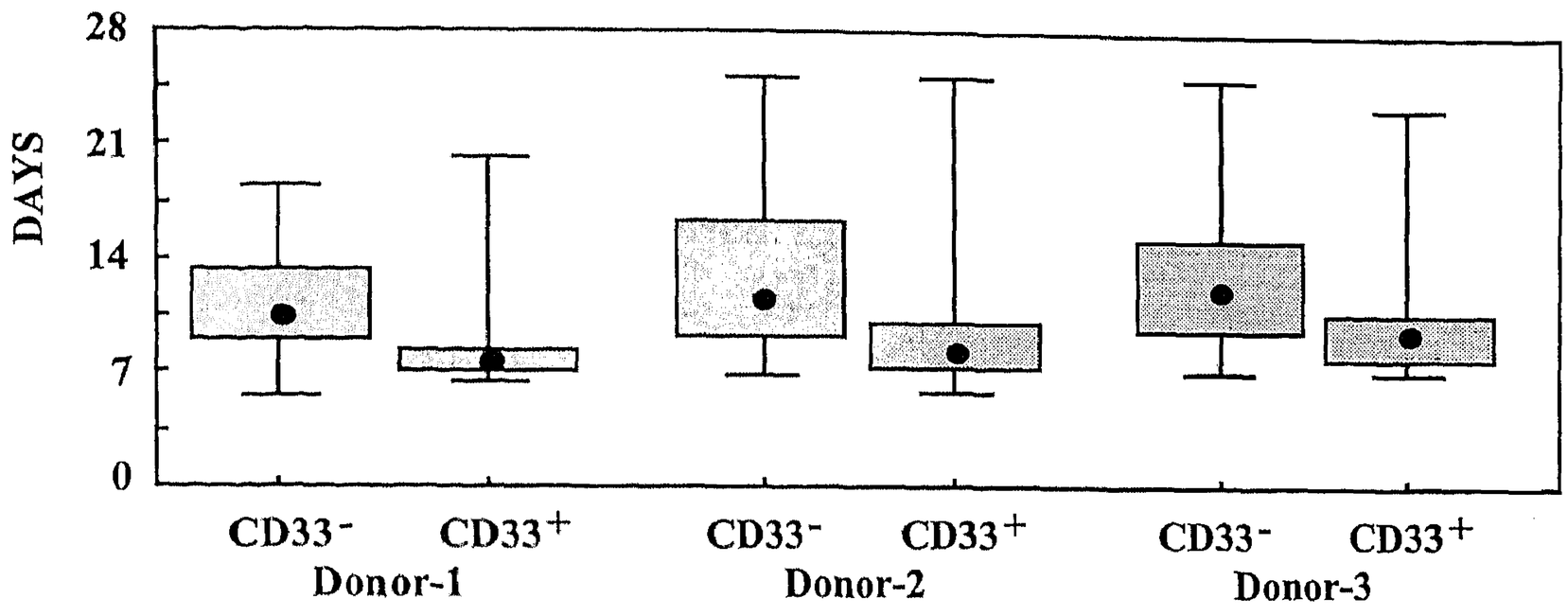

FIG. 4. Comparison of growth delay of CD34+/CD13+/CD33+ and CD34+/CD13+/CD33− cells in 3 different normal bone marrow donors measured by image analysis. Mean delay of growth initiation was 2.6–3.1 days, Mann-Whitney, $P < 0.001$.

started at size = 1 at zero time point, this point is ignored in the panels. Figure 3C shows examples of curves of non-growing wells, with less than 10 cells. Noise measured in the non-growing wells reflected small objects, sometimes in a different focal plane than the sorted cells.

Parametrization

The curve of a well showing growth expressed three phases: the start with a no-growth immediately after sorting, the log growth phase, and finally a plateau. The kinetics of the log growth phase was parametrized with the two parameters, growth rate and growth delay, at 600 cells. Figure 4 shows that in all 3 tested normal bone marrow donors a significant delay in growth initiation (Mann-Whitney, $P < 0.001$) was expressed with a median shift of 2.6–3.1 days. Thus within the CD34+/CD33− fraction there is a larger heterogeneity in the time point where growth is initiated, which means that only a fraction of progenitors starts to grow at a later time point.

DISCUSSION

In the current study, image analysis was applied for automatic enumeration of individual cells in single cell derived cultures in 96-well plates. The blast-like, round-shaped cells in bright-phase contrast could be easily detected. This allowed a highly specific segmentation routine, thus reducing the risk of false negatives. Fortunately, the cells keep this blast-like appearance in the proliferative phase and change in morphology during differentiation thereafter. Once the cells start to differentiate, tracking in bright-phase contrast becomes less accurate. The advantage of the bright-phase contrast as a method to detect the single cells is the avoidance of vital dyes. The round bottom well centers the single sorted cell as well as the successive stages of the growing colony in the middle of the well. In flat bottom wells it appeared very difficult to detect single cells at 50× magnification. Once a few single cells are present, focusing becomes easy and objects can be traced reliably for repeated measurements. The efficiency was equal for 50× and 100× magnification. As the lowest magnification had the least edge loss and the largest field size, 50× was the preferred magnification. Large colonies (>5,000 cells) tended to pass the edges (0.7 × 0.7 mm view) and cells started to pile up. The described method does not provide exact

information on the final size of the larger colonies, but it is accurate to determine the log growth phase. Cells that divided 1–3-fold, formed clusters of less than 10 cells, and then stopped growing were not always detected correctly. One explanation was that these cells often become pycnotic and lose the characteristic appearance in bright phase-contrast microscopy. To reduce false positive objects the media were filtered through a 0.2-μm Millipore filter, which removes small particles. More than 10 blast-like cells were detected with a high specificity and sensitivity. The accuracy of the segmentation routine in detecting the individual cells in growing colonies was shown to be highly significantly correlated with manual counting.

To show the feasibility of the method, two subpopulations of CD34+ human bone marrow cells, CD13+/CD33+ and CD13+/CD33−, were compared in growth behavior. The somewhat more primitive CD13+/33− cells were shown to be significantly delayed in growth initiation while the growth rate during log phase was similar as for the CD13+/33+. The growth delay most probably is due to the non-cycling status of the more primitive progenitors. Although we observed growth delay in previous single-cell experiments, since some progenitors started to divide only after 7 or more days, image analysis was allowed to quantitate the growth delay. We showed that once growth was initiated, the rate of proliferation was similar using the same growth factors and culture conditions. The doubling time of the fast-growing colonies was around 12–20 h. From previous observations it was known that the cells that showed growth delay remained in their single cells state for 7 or more days. For that reason the plotted curves were not forced through the zero time point. Simply plotting the curves through the zero time point ignores the difference between delayed growth initiation and a slower growth ratio.

The advantage over previous methods of image analysis is that the actual number of living cells is counted, not estimated by colony areas. Xu-van Opstal et al. counted the actual number of living cells in cultures but not individual growing colonies (9). Dow et al. developed a system of image analysis based on Hoechst staining, image analysis of isolated cells as well as aggregate; however, it cannot be used in sequential measurements of fast-growing individual progenitor cells (1). Single-cell sorting guarantees accurate seeding and thus determination of plating efficiency. If plated in agar, growing colonies can merge or disperse, the latter being a problem in bone marrow colonies. Both processes complicate accurate tracing of growth.

The described method might be useful in the study of different growth factors or a combination of growth factors and inhibitors on the proliferative rate and initiation of growth. It can also be applied to cell lines growing in liquid, provided they grow in a single-cell system. Also growth rates of different progenitors, normal as well as leukemic, can be compared.

LITERATURE CITED

1. Dow AI, Shafer SA, Kirkwood JM, Mascari RA, Waggoner AS. Automatic multiparameter fluorescence imaging for determining lymphocyte phenotype and activation status in melanoma tissue sections. Cytometry 25:71–81, 1996.
2. Grunwald J: Time-lapse video microscopic analysis of cell proliferation, motility and morphology: Applications for cytopathology and pharmacology. BioTechniques 5:680–687, 1987.
3. Haudenschild CC, Grunwald J: Proliferative heterogeneity of vascular smooth muscle cells and its alteration by injury. Exp Cell Res 157:364–370, 1985.
4. Kahn E, Benard J, Di Paola R: The use of an image analyser in human tumour clonogenic assays. Cytometry 7:313–317, 1986.
5. Kressner BE, Morton RR, Martens AE, Salmon SE, Von Hoff DD, Soehnlen B: Use of an image analysis system to count colonies in stem cell assays of human tumors. Prog Clin Biol Res 48:179–193, 1980.
6. Malmberg M, Slocum HK, Rustum YM: Growth slow-down and growth arrest of human colon carcinoma cells HCT-8 in vitro after exposure to 5-fluoro-2′-deoxyuridine. Cell Prolif 26:291–303, 1993.
7. Raymakers RA, Slocum HK, Minderman, H, Malmberg M, Rustum YM: Characterization of tumor cell heterogeneity of a murine leukemia cell line (L1210) in response to arabinosylcytosine: Quantitation using a computerized image analysis system. Exp Hematol 21:602–607, 1993.
8. Slocum HK, Malmberg M, Greco WR, Parsons JC, Rustum YM: The determination of growth rates of individual colonies in agarose using high-resolution automated image analysis. Cytometry 11:793–801, 1990.
9. Xu-van Opstal WY, Ranger C, Lejeune O, Forgez P, Boudin H, Biseonte JC, Rostene W. Automated image analyzing system for the quantitative study of living cells in culture. Microsc Res Tech 28:410–417, 1994.